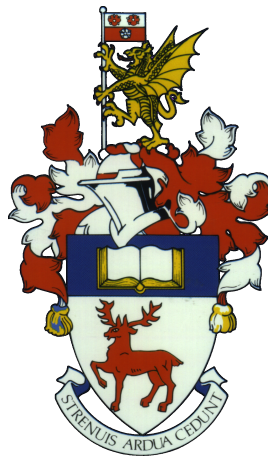


1 **Novel Approaches to Fast Filling of Hydrogen Cylinders**

2 Pau Miquel Mir
 28023668

Supervisor: Dr. Edward Richardson
Word count: 1657

3 May 2018



4 This report is submitted in partial fulfillment of the requirements for the MEng Mechanical
5 Engineering, Faculty of Engineering and the Environment, University of Southampton.

6

Declaration

7

I, Pau Miquel Mir, declare that this thesis and the work presented in it are my own and has been generated by me as the result of my own original research. I confirm that:

8

9

1. This work was done wholly or mainly while in candidature for a degree at this University;

10

2. Where any part of this thesis has previously been submitted for any other qualification at this University or any other institution, this has been clearly stated;

11

12

3. Where I have consulted the published work of others, this is always clearly attributed;

13

4. Where I have quoted from the work of others, the source is always given. With the exception of such quotations, this thesis is entirely my own work;

14

15

5. I have acknowledged all main sources of help;

16

6. Where the thesis is based on work done by myself jointly with others, I have made clear exactly what was done by others and what I have contributed myself;

17

18

7. None of this work has been published before submission.

19

Acknowledgements

20

I want to thank my advisor, Dr. Edward Richardson, for his time and dedication.

21

Furthermore, I would like to thank Vishagen Ramasamy for his initial work upon which this paper builds.

22

23

I also want to thank my parents, for their constant support and for proofreading the paper.

24

Abstract

25

This is the abstract.

26	Contents	
27	Declaration	i
28	Acknowledgements	ii
29	Abstract	iii
30	Acronyms	vi
31	1 Introduction	1
32	1.1 Purpose of the investigation	1
33	1.2 Outline of the investigation	1
34	2 Background	2
35	2.1 Vehicles and objectives	2
36	2.1.1 Material constraints	2
37	2.2 Previous work	2
38	2.2.1 Modeling Work	2
39	2.2.2 Experimental work	2
40	2.2.3 Analysis	3
41	2.3 Cylinder filling models	3
42	2.3.1 Zonal	3
43	2.3.2 Multidimensional	3
44	2.4 Heat transfer models	3
45	2.4.1 Impinging jet	3
46	2.4.2 Pipe flow	3
47	2.4.3 Turbulent Jets	4
48	2.5 Methodology	4
49	2.5.1 Optimization	4
50	2.5.2 Non-dimensioning	4
51	2.5.3 Numerical methods	4
52	3 Formulation	5
53	3.1 Heat transfer across cylinder	5
54	3.2 Gas flow into cylinder	5
55	3.3 Hysteresis	5
56	3.4 Throttling	5
57	3.5 Optimization	5
58	Appendices	6
59	A Filling Code	6

60 **References**

10

61 **Acronyms**

62 **CFD** Computational Fluid Dynamics

1 Introduction

1.1 Purpose of the investigation

Hydrogen is a very promising alternative fuel for the future, mainly due to the absence of greenhouse emissions when burning it. In this regard, it is superior to current petroleum-, and more generally, carbon-based fueling systems. However, air pollution is a negative externality associated with carbon-based fuels, as it is a cost to a third party (in this case, society as a whole) that is not accounted for in the price of the good. By definition, the negative consequences of polluting the air are not accounted for in the price of carbon vehicles, and therefore will have little influence on a consumer's choice. Thus, if hydrogen is to succeed as an alternative to carbon fuels, it is essential that its use be as - if not more - convenient than traditional fuel.

One of the main aspects that currently lags behind traditional fuel is the refueling experience. Given that refueling hydrogen involves its compression, there is a significant rise in temperature, which must be kept below certain standards (358K as per SAE J2601). This in turn leads to long refueling times, potentially lasting more than five minutes, which is cumbersome for users. Therefore, it is of prime importance to research and develop systems that enable the faster refueling of hydrogen cylinders. To this end, this project will build upon a model of filling a hydrogen cylinder which has already been developed by members of the department in order to analyse novel methods of improving fill times.

1.2 Outline of the investigation

One of the current solutions to improve fill times involves cooling the hydrogen before filling the cylinder as to keep it below the maximum temperature. However, this is quite expensive, both in energy terms and in economic terms. Consequently, the aim of this project is to continue exploring several of the options available to reduce fill times and simultaneously reduce the energy consumption of the process, thus improving both convenience for users and energy efficiency of the fueling stations. Indeed, by building upon the existing cylinder model several options shall be considered, namely: refrigeration, flow regulation, heat sink usage, active cooling, heat pipe usage, and phase change materials. From here, several options are open to further deepen or potentially broaden the investigation. An attempt to further simplify the model can be made, perhaps even reducing it to a simple algebraic relationship. Also, the model would benefit from FEA validation to aid our understanding of the heat transfer in the structure. This would go hand in hand with analyzing the temperature of the structure, and see how close this matches the gas temperature. Indeed, if the structure is at a much lower temperature than the gas, the case can be made that the current regulations are slightly erroneous, as they are meant to protect the materials of the structure, but instead regulate the gas temperature.

Update with
actual options
considered at
end of project

2 Background

2.1 Vehicles and objectives

We must firstly consider what real-world relevance of this project is. As explained in Section 1, the hydrogen cylinders being considered are for road vehicles.

2.1.1 Material constraints

The main reason that a problem exists, and consequently this paper (and much other work) is being undertaken, is the material limitations that exist in hydrogen cylinders. Indeed, the cylinders that are used for high pressure scenarios such as the one we are presented with, are constructed with a composite material such as carbon fibre or glass/aramid fibre. In addition, they have a liner that is made out of metal, typically aluminum, in Type III cylinders, and out of a thermoplastic material for Type IV cylinders. Of concern is the composite material, as the polymer matrix cannot withstand high temperatures, and as such the material properties of the cylinder will begin to degrade. The specific temperature at which this occurs is usually around the glass transition temperature of the epoxy, where the thermosetting polymer changes from a hard "glassy" state to a more compliant "rubbery" state.

2.2 Previous work

We must first establish a baseline of previous work that has been conducted in this field, and subsequently analyze the shortcomings that exist in order to direct the research.

2.2.1 Modeling Work

A large amount of research has been conducted using multidimensional analysis, especially using Computational Fluid Dynamics (CFD). Indeed, there is myriad papers describing different methods and setups, such as Dicken and Mérida's work, which uses the standard k- ϵ turbulence model and the Redlich-Kwong real gas equation of state for real gas properties [1]. Some of these models use more advanced property models, such as the model presented by Zhao et al., which employs REFPROP (see Section 2.5.3) in order to have more precise real gas properties [2].

2.2.2 Experimental work

Several papers describe experimental work that has been conducted regarding the fast-filling of hydrogen cylinders, in particular comparing the results to simulations. Dicken and Mérida's work indicates that the temperature inside the cylinder is rather uniform [3]. This claim is not, however supported by the work of Zheng et al nor that of Woodfield et al [4], wherein large discrepancies among gas temperatures in different regions of the cylinder are found.

{sec:experimental_w

Citation

2.2.3 Analysis

The simulation work that has been conducted can be, in broad terms, divided into complex CFD models and more simplified 0-dimensional models. It is important to analyze the difference between these two systems. The main advantage of reduced dimension models is that they are much less computationally expensive. This, in turn, means it can be incorporated as part of a larger analysis, in which it must be run multiple times, such as optimization routines or probabilistic whole station models.

Reduced dimension models assume a constant gas temperature, which, as outlined in Section 2.2.2, is supported by some experimental work, but refuted by others. For this reason, more research should be conducted to validate the uniform gas temperature approximation.

2.3 Cylinder filling models

Several ways of modeling the cylinder can be considered when analysing their filling, with varying complexity and accuracy.

2.3.1 Zonal

A zonal model, also referred to as a 0-dimensional model, refers to models that consider the gas inside the cylinder as the control volume, with homogenous properties. This allows for simpler calculations,

2.3.2 Multidimensional

More complex multidimensional models can be created, either 2D axisymmetric models or full 3D models. 2D models will not include the effects of gravity or buoyancy, but

2.4 Heat transfer models

In order to successfully analyze the behaviour of the system as a whole we must consider several local heat transfer methods that occur at different places inside of the cylinder.

2.4.1 Impinging jet

The first behaviour that we will consider is that of an impinging jet of fluid onto a surface.

FIGURE 1: Impinging jet

2.4.2 Pipe flow

A second behaviour that we will consider is that of pipe flow. This behaviour has been the focus of much research, as it is arguably the most common mode of heat transfer that occurs in most fluid systems.

2.4.3 Turbulent Jets

Lastly, we must also consider turbulent jets, as there will be such a situation at the exit of the nozzle.

2.5 Methodology

Throughout the analysis that will be conducted several methods and techniques will be used. These are described in this section.

2.5.1 Optimization

Fill Section
once work on
optimization
starts.

2.5.2 Non-dimensioning

One of the fundamental principals used throughout this paper, and indeed, throughout engineering, is that of non-dimensioning. By operating using non-dimensional parameters such as the Reynolds number $Re = \frac{\rho u L}{\mu}$ or the Prandtl number $Pr = \frac{c_p \mu}{k}$ solving problems involving differential equations becomes simplified. Also, the analysis becomes much more general, and can be scaled.

2.5.3 Numerical methods

{sec:numerical_meth

Integrating ODEs An central part of solving unsteady heat transfer problems involves integrating ODEs, as will be seen in Section 3. One of the simplest methods available, both conceptually and in terms of ease of implementing in code, is forward Euler time integration. It can be informally described as follows: given a function that can be defined by:

$$y'(t) = f(t, y(t)), \quad y(t_0) = y_0 \quad (2.1)$$

we can compute the approximate shape of the function given the initial point and finding the slope of the curve for small intervals. Indeed, from the initial point, we can find the tangent of the curve at that point, and take a small step along that tangent until arriving at the next point, where the procedure can be repeated. Denoting the step size h , we can express forward Euler time integration as:

$$y_{n+1} = y_n + hf(t_n, y_n) \quad (2.2)$$

{sec:property_model

Property models As the gases that are being treated in this report are at very high pressures, ideal gas approximations are inaccurate, and thus real gas properties must be employed. To this end, property models must be used, which can determine any gas property from two other independent properties.

The property model that will be employed throughout this analysis is REFPROP, a tool developed by the National Institute of Standards and Technology [5]. It uses values of critical and triple points together with equations for the thermodynamic and transport properties to calculate the state points of fluids.

3 Formulation

3.1 Heat transfer across cylinder

The main mode of heat transfer that occurs in the cylinder and that will be used throughout this report is heat conduction through the wall of the cylinder. This is modeled using:

$$\frac{\partial T}{\partial t} = \alpha \frac{\partial^2 T}{\partial x^2} \quad (3.1)$$

where α is the thermal diffusivity, which is defined by :

$$\alpha = \frac{k}{\rho c} \quad (3.2)$$

where k is the material's thermal conductivity, ρ is the density of the material, and c is the specific heat capacity of the material.

This differential equation will be solved using forward Euler time integration as described in Section 2.5.3

3.2 Gas flow into cylinder

The nozzle and corresponding gas flow will be modeled using isentropic relations, and then a discharge coefficient relationship will be used to find the approximate real values. Indeed, the isentropic Reynold's number is first calculated as follows:

$$\text{Re}_{\text{ideal}} = \frac{\rho_{\text{exit}} d_{\text{inlet}} u_{\text{exit}}}{\mu_{\text{exit}}} \quad (3.3)$$

where ρ_{exit} , d_{inlet} , u_{exit} , and μ_{exit} are determined using real gas models as described in Section 2.5.3. In order to find the real mass flow an empirical discharge coefficient is employed:

$$\text{CD} = \frac{\dot{m}_{\text{in}}}{\dot{m}_{\text{ideal}}} = A + B \text{Re}_{\text{ideal}} \quad (3.4)$$

A discharge coefficient must be used to account for the formation of a boundary layer inside the inlet tube. The empirical model that was used was obtained from [1], and uses the following values:

$$A = 0.938, \quad B = -2.71 \quad (3.5)$$

3.3 Hysteresis

3.4 Throttling

3.5 Optimization

206 **Appendices**207 **A Filling Code**

{app:filling_code}

```

1 %Author: Vishagen Ramasamy
2 %Date: -
3
4 % Copyright University of Southampton 2017.
5 % No warranty either expressed or implied is given to the results produced
6 % by this software. Neither the University, students or its employees
7 %accept any responsibility for use of or reliance on results produced by
8 %this software.
9
10 %% script that computes the filling of the tank(s)
11 %% Importing the pressure and temperature profile at the entrance of the delivery pipe from Dicken and Merida
12 % and calculating the stagnation enthalpy and entropy
13
14 for j = 1:maxt
15     time(j+1) = (j)*dt; % Time as filling proceeds
16     for i = 1:tank_number
17         % Select inlet pressure / temperature profile based on user input
18         if blnUseStandardData == 1
19             % Constant inlet pressure profile
20             P_inlet(i,j+1) = ConstPressKPa;
21         else
22             % Read inlet pressure profile from specified file
23             P_inlet(i, j+1) = interp1(InletPressureData(:,1),InletPressureData(:,3), dt*j);
24         end
25
26         if blnUseStandardData == 1
27             %Temp_inlet(i,j+1) = interp1(time_in, temp_in, dt*j); % Temperature profile after the first 1.35 s
28             Temp_inlet(i, j+1) = ConstTempK;
29         else
30             % Read inlet temperature profile from specified file
31             Temp_inlet(i, j+1) = interp1(InletTempData(:,1), InletTempData(:,3), dt*j);
32         end
33
34         h_inlet(i,j+1) = refpropm('H','T',Temp_inlet(i,j+1),'P',P_inlet(i,j+1),Fluid{i}, refpropdir); % R
35         entropy_inlet(i,j+1) = refpropm('S','T',Temp_inlet(i,j+1),'P',P_inlet(i,j+1),Fluid{i}, refpropdir); % R
36
37         %% Determine which pressure to use at the exit of the delivery pipe which is dependent upon the number o
38
39         if l_d(i) > 3 && blnOneZone{i} == 0 % The length-to-diameter ratio of the tank(s) determines th
40             Pressure_exit = P_gas_zone1{i}(j); % The pressure at the exit of the delivery pipe is equal to the
41         else
42             Pressure_exit = P_gas(i,j); % The pressure at the exit of the delivery pipe is equal to the
43         end
44
45         if (P_inlet(i,j+1) > Pressure_exit) % condition for filling of tank(s)
46             sound_exit(i,j+1) = refpropm('A','P',Pressure_exit,'S',entropy_inlet(i,j+1),Fluid{i}, refpropdir);
47             h_static_exit(i,j+1) = refpropm('H','P',Pressure_exit,'S',entropy_inlet(i,j+1),Fluid{i}, refpropdir);
48             visc_exit(i,j+1) = refpropm('V','P',Pressure_exit,'S',entropy_inlet(i,j+1),Fluid{i}, refpropdir);
49             mach_exit(i,j+1) = sqrt(2*(h_inlet(i,j+1)-h_static_exit(i,j+1))/sound_exit(i,j+1)^2); % Calculates
50
51             %% If Mach number is greater than one, the exit pressure is greater than the pressure within the tan
52             % is incrementally increased and iterated in a while loop until mach number is equal to one
53
54             Inlet_entropy = entropy_inlet(i,j+1);
55             Inlet_stagnation_enthalpy = h_inlet(i,j+1);
56             P_guess = Pressure_exit;
57
58             if mach_exit(i,j+1) > 1
59                 Pressure_exit = find_exit_pressure(Inlet_stagnation_enthalpy,Inlet_entropy,Fluid{i},P_guess, ref
60                 sound_exit(i,j+1) = refpropm('A','P',Pressure_exit,'S',Inlet_entropy,Fluid{i}, refpropdir);
61                 h_static_exit(i,j+1) = refpropm('H','P',Pressure_exit,'S',Inlet_entropy,Fluid{i}, refpropdir);

```

```

62         visc_exit(i,j+1) = refpropm('V','P',Pressure_exit,'S',Inlet_entropy,Fluid{i}, refprop
63         mach_exit(i,j+1) = sqrt(2*(h_inlet(i,j+1)-h_static_exit(i,j+1))/sound_exit(i,j+1)^2)
64     end
65
66     %% Calculation of the mass flow rate into the tank(s)
67
68     rho_exit(i,j+1) = refpropm('D','P',Pressure_exit,'S',Inlet_entropy,Fluid{i}, refpropdir)
69     vel_exit(i,j+1) = mach_exit(i,j+1)*sound_exit(i,j+1);
70     Re_exit_isentropic(i,j+1) = rho_exit(i,j+1) *d_inlet*vel_exit(i,j+1)/visc_exit(i,j+1);
71     cd(i,j+1) = 1 + J/(Re_exit_isentropic(i,j+1)^(0.25));
72     mfr(i,j+1) = cd(i,j+1)*rho_exit(i,j+1)*vel_exit(i,j+1)*A_inlet;
73     Re_entrance_actual(i,j+1) = 4*mfr(i,j+1)/(pi*d_inlet*visc_exit(i,j+1));
74     dM_inlet = mfr(i,j+1)*dt;
75 end
76
77 %% Heat transfer calculations & caluculations of the thermodynamic properties of the gas in t
78 if l_d(i) <= 3 | blnOneZone{i} == 1
79
80     Nus(i,j+1) = a_1*Re_entrance_actual(i,j+1)^(b_1); % Nusselt number a
81     k_gas(i,j+1) = refpropm('L','T',Temp_gas(i,j),'P',P_gas(i,j),Fluid{i}, refpropdir); % T
82     heat_coef_forced(i,j+1) = Nus(i,j+1)*k_gas(i,j+1)/d_tank(i); % Calculation of t
83
84     if Inner_wall_boundary(i) == 1
85         Qsurf(i,j+1) = -dt*surf_area(i)*heat_coef_forced(i,j+1)*(Temp_gas(i,j)-Inner_temp_wa
86     else
87         Qsurf(i,j+1) = -dt*surf_area(i)*heat_coef_forced(i,j+1)*(Temp_gas(i,j)-Temp_wall{i}(
88         Temp_wall{i}(1,j+1) = Temp_wall{i}(1,j) + CFL_liner(i)*(Temp_wall{i}(2,j)- Temp_wall{
89
90         if Outer_wall_boundary(i)==1
91             Temp_wall{i}(number_of_gridpoints(i),j+1) = Outer_temp_wall_isothermal(i);
92         else
93             Temp_wall{i}(number_of_gridpoints(i),j+1) = Temp_wall{i}(number_of_gridpoints(i)
94         end
95         % Computation of the temperature of the struture of the tank(s)
96         for k=2:number_of_gridpoints(i)-1
97             if (k>=2)&&(k<=int_pt_liner_laminate(i)-1)
98                 Temp_wall{i}(k,j+1) = Temp_wall{i}(k,j)+CFL_liner(i)*(Temp_wall{i}(k+1,j)-2*
99             elseif (k>=int_pt_liner_laminate(i)+1)&&(k<=number_of_gridpoints(i)-1)
100                 Temp_wall{i}(k,j+1) = Temp_wall{i}(k,j)+CFL_laminate(i)*(Temp_wall{i}(k+1,j)
101             else
102                 Temp_wall{i}(k,j+1) = (cond_laminate(i)*(Temp_wall{i}(k+1,j)+CFL_laminate(i)
103             end
104         end
105     end
106     m_gas(i,j+1) = m_gas(i,j) + dM_inlet; % Mas
107     Ugas(i,j+1)=Ugas(i,j)+Qsurf(i,j+1)+h_inlet(i,j+1)*dM_inlet; % Int
108     u_gas(i,j+1)= Ugas(i,j+1)/m_gas(i,j+1); % Spe
109     rho_gas(i,j+1)=m_gas(i,j+1)/vol_tank(i); % Den
110     P_gas(i,j+1) = refpropm('P','D',rho_gas(i,j+1),'U',u_gas(i,j+1),Fluid{i}, refpropdir);
111     Temp_gas(i,j+1) = refpropm('T','D',rho_gas(i,j+1),'U',u_gas(i,j+1),Fluid{i}, refpropdir)
112
113 else
114     Re_compression(i,j+1) = Re_entrance_actual(i,j+1)*(d_inlet/d_tank(i)); % Rey
115
116     Nus_zone1{i}(j+1) = a_1*Re_entrance_actual(i,j+1)^(b_1); % Nus
117     Nus_zone2{i}(j+1) = c_1*Re_compression(i,j+1)^(d_1); % Nus
118
119     k_gas_zone1{i}(j+1) = refpropm('L','T',Temp_gas_zone1{i}(j),'P',P_gas_zone1{i}(j),Fluid
120     k_gas_zone2{i}(j+1) = refpropm('L','T',Temp_gas_zone2{i}(j),'P',P_gas_zone2{i}(j),Fluid
121
122     heat_coef_forced_zone1{i}(j+1) = Nus_zone1{i}(j+1)*k_gas_zone1{i}(j+1)/d_tank(i);
123     heat_coef_forced_zone2{i}(j+1) = Nus_zone2{i}(j+1)*k_gas_zone2{i}(j+1)/l_zone2_total(i)
124
125     % Step 1. Equating the respecting values of zone 1 and zone 2 to
126     % matrices with 'similar' names
127

```

```

128     Vgas(1)=volume_zone1(i);
129     Vgas(2)=volume_zone2(i);
130     Mgas(1)=m_gas_zone1{i}(j);
131     Mgas(2)=m_gas_zone2{i}(j);
132     Ugas_twozone(1)=u_gas_zone1{i}(j)*Mgas(1);
133     Ugas_twozone(2)=u_gas_zone2{i}(j)*Mgas(2);
134     Asurf(1)=surface_area_zone1(i);
135     Asurf(2)=surface_area_zone2(i);
136     Tgas(1)=Temp_gas_zone1{i}(j);
137     Tgas(2)=Temp_gas_zone2{i}(j);
138     if Inner_wall_boundary(i) == 1
139         Twall(1,1)=Inner_temp_wall_isothermal(i);
140         Twall(2,1)=Inner_temp_wall_isothermal(i);
141     else
142         Twall(1,1)=Temp_wall_zone1{i}(1,j);
143         Twall(2,1)=Temp_wall_zone2{i}(1,j);
144     end
145     % Step 2: apply the change of internal energy due to heat transfer and mass
146     % input through nozzle:
147
148     dM_inlet = mfr(i,j+1)*dt;
149
150     Qsurf(1)=- dt*Asurf(1)*(heat_coef_forced_zone1{i}(j+1))*(Tgas(1)-Twall(1,1));
151     Qsurf(2)=- dt*Asurf(2)*(heat_coef_forced_zone2{i}(j+1))*(Tgas(2)-Twall(2,1));
152
153     Ugas_twozone(1)=Ugas_twozone(1)+Qsurf(1)+h_inlet(i,j+1)*dM_inlet;
154     Ugas_twozone(2)=Ugas_twozone(2)+Qsurf(2);
155
156     Mgas(1)=Mgas(1)+dM_inlet;
157     Mgas(2)=Mgas(2);
158
159     for m=1:2
160         hgas(m)=refpropm('H','D',Mgas(m)/Vgas(m),'U',Ugas_twozone(m)/Mgas(m),Fluid{i}, refpropdir);
161     end
162
163
164     % Step 2: Find the amount of mass that needs to be transferred from zone 1
165     % to zone 2 to equalise their pressure
166     % (we assume forward Euler integration, therefore we use the specific
167     % enthalpies h from the start of the timestep. We provide enthalpies for
168     % both zones in case the flow gets reversed).
169
170     dM_guess = dM_inlet*(volume_zone2(i)/(volume_zone1(i)+volume_zone2(i))) ;
171     dM_12 = find_dM_12(hgas,Vgas,Mgas,Ugas_twozone,Fluid{i},dM_guess, refpropdir);
172
173     % Step 3: Apply this change to the mass and update all properties:
174
175     m_gas_zone1{i}(j+1)=Mgas(1)-dM_12;
176     m_gas_zone2{i}(j+1)=Mgas(2)+dM_12;
177
178     u_gas_zone1{i}(j+1)=(Ugas_twozone(1)-max(0,dM_12)*hgas(1)-min(0,dM_12)*hgas(2))/m_gas_zone1{i}(j+1);
179     u_gas_zone2{i}(j+1)=(Ugas_twozone(2)+max(0,dM_12)*hgas(1)+min(0,dM_12)*hgas(2))/m_gas_zone2{i}(j+1);
180
181     rho_gas_zone1{i}(j+1)=m_gas_zone1{i}(j+1)/volume_zone1(i);
182     rho_gas_zone2{i}(j+1)=m_gas_zone2{i}(j+1)/volume_zone2(i);
183
184     Temp_gas_zone1{i}(j+1)=refpropm('T','D',rho_gas_zone1{i}(j+1),'U', u_gas_zone1{i}(j+1),Fluid{i}, refpropdir);
185     Temp_gas_zone2{i}(j+1)=refpropm('T','D',rho_gas_zone2{i}(j+1),'U', u_gas_zone2{i}(j+1),Fluid{i}, refpropdir);
186
187     P_gas_zone1{i}(j+1)=refpropm('P','D',rho_gas_zone1{i}(j+1),'U', u_gas_zone1{i}(j+1),Fluid{i}, refpropdir);
188     P_gas_zone2{i}(j+1)=refpropm('P','D',rho_gas_zone2{i}(j+1),'U', u_gas_zone2{i}(j+1),Fluid{i}, refpropdir);
189
190     m_gas(i,j+1) = m_gas_zone1{i}(j+1) + m_gas_zone2{i}(j+1);
191     rho_gas(i,j+1) = m_gas(i,j+1)/vol_tank(i);
192     u_gas(i,j+1)= (u_gas_zone1{i}(j+1)*m_gas_zone1{i}(j+1)+ u_gas_zone2{i}(j+1)*m_gas_zone2{i}(j+1))/m_gas(i,j+1);
193     Ugas(i,j+1) = u_gas(i,j+1)*m_gas(i,j+1);

```



```

194     Temp_gas(i,j+1) = refpropm('T','D',rho_gas(i,j+1),'U',u_gas(i,j+1),Fluid{i}, refpropdir
195     P_gas(i,j+1) = refpropm('P','D',rho_gas(i,j+1),'U',u_gas(i,j+1),Fluid{i}, refpropdir);
196
197     if Inner_wall_boundary(i) == 1
198         Qsurf_zone1{i}(j+1) = -dt*surface_area_zone1(i)* heat_coef_forced_zone1{i}(j+1)*(Tem
199         Qsurf_zone2{i}(j+1) = -dt*surface_area_zone2(i)* heat_coef_forced_zone2{i}(j+1)*(Tem
200     else
201         Qsurf_zone1{i}(j+1) = -dt*surface_area_zone1(i)* heat_coef_forced_zone1{i}(j+1)*(Tem
202         Qsurf_zone2{i}(j+1) = -dt*surface_area_zone2(i)* heat_coef_forced_zone2{i}(j+1)*(Tem
203
204         Temp_wall_zone1{i}(1,j+1) = Temp_wall_zone1{i}(1,j)+ CFL_liner(i)*(Temp_wall_zone1{i}
205         Temp_wall_zone2{i}(1,j+1) = Temp_wall_zone2{i}(1,j)+ CFL_liner(i)*(Temp_wall_zone2{i}
206
207         if Outer_wall_boundary(i)==1
208             Temp_wall_zone1{i}(number_of_gridpoints(i),j+1) = Outer_temp_wall_isothermal(i);
209             Temp_wall_zone2{i}(number_of_gridpoints(i),j+1) = Outer_temp_wall_isothermal(i);
210         else
211             Temp_wall_zone1{i}(number_of_gridpoints(i),j+1) = Temp_wall_zone1{i}(number_of_g
212             Temp_wall_zone2{i}(number_of_gridpoints(i),j+1) = Temp_wall_zone2{i}(number_of_g
213         end
214         % Computation of the temperature of the struture of the tank(s)
215         for k=2:number_of_gridpoints(i)-1
216             if (k>=2)&&(k<=int_pt_liner_laminate(i)-1)
217                 Temp_wall_zone1{i}(k,j+1) = Temp_wall_zone1{i}(k,j)+CFL_liner(i)*(Temp_wall_
218                 Temp_wall_zone2{i}(k,j+1) = Temp_wall_zone2{i}(k,j)+CFL_liner(i)*(Temp_wall_
219             elseif (k>=int_pt_liner_laminate(i)+1)&&(k<=number_of_gridpoints(i)-1)
220                 Temp_wall_zone1{i}(k,j+1) = Temp_wall_zone1{i}(k,j)+CFL_laminate(i)*(Temp_wa
221                 Temp_wall_zone2{i}(k,j+1) = Temp_wall_zone2{i}(k,j)+CFL_laminate(i)*(Temp_wa
222             else
223                 Temp_wall_zone1{i}(k,j+1) = (cond_laminate(i)*(Temp_wall_zone1{i}(k+1,j)+CFL
224                 Temp_wall_zone2{i}(k,j+1) = (cond_laminate(i)*(Temp_wall_zone2{i}(k+1,j)+CFL
225             end
226         end
227     end
228
229     end
230
231     end
232 end

```

References

- [1] C. J. B. Dicken and W. Mérida, “Modeling the Transient Temperature Distribution within a Hydrogen Cylinder during Refueling”, *Numerical heat transfer, part a: Applications*, vol. 53, no. 7, pp. 685–708, Nov. 2007, ISSN: 1040-7782. DOI: 10.1080/10407780701634383. [Online]. Available: <http://www.tandfonline.com/doi/abs/10.1080/10407780701634383>
- [2] Y. Zhao, G. Liu, Y. Liu, J. Zheng, Y. Chen, L. Zhao, J. Guo, and Y. He, “Numerical study on fast filling of 70 MPa type III cylinder for hydrogen vehicle”, *International journal of hydrogen energy*, vol. 37, no. 22, pp. 17 517–17 522, 2012, ISSN: 0360-3199. DOI: <https://doi.org/10.1016/j.ijhydene.2012.03.046>. [Online]. Available: <http://www.sciencedirect.com/science/article/pii/S0360319912006477>.
- [3] C. Dicken and W. Mérida, “Measured effects of filling time and initial mass on the temperature distribution within a hydrogen cylinder during refuelling”, *Journal of power sources*, vol. 165, no. 1, pp. 324–336, Feb. 2007, ISSN: 03787753. DOI: 10.1016/j.jpowsour.2006.11.077. [Online]. Available: https://www.engineeringvillage.com/share/document.url?mid=cpx%7B%5C_%7D30c221110dfeaa71cM69f92061377553%7B%5C%7Ddatabase=cpx.
- [4] P. L. WOODFIELD, M. MONDE, and T. TAKANO, “Heat Transfer Characteristics for Practical Hydrogen Pressure Vessels Being Filled at High Pressure”, *Journal of thermal science and technology*, vol. 3, no. 2, pp. 241–253, 2008. DOI: 10.1299/jtst.3.241.
- [5] E. W. Lemmon, M. L. Huber, and M. O. McLinden, *NIST Standard Reference Database 23: Reference Fluid Thermodynamic and Transport Properties-REFPROP, Version 9.1*, National Institute of Standards and Technology, 2013. DOI: <http://dx.doi.org/10.18434/T4JS3C>. [Online]. Available: <https://www.nist.gov/srd/refprop>.

231 **Todo list**

232	Update with actual options considered at end of project	1
233	Citation	2
234	Fill Section once work on optimization starts.	4
235	Citation	5